THE ORIGIN OF POSTFLARE LOOPS

N. R. Sheeley, Jr., H. P. Warren, and Y.-M. Wang

E. O. Hulburt Center for Space Research, Naval Research Laboratory, Washington, DC 20375-5352;
sheeley@spruce.nrl.navy.mil, hwarren@nrl.navy.mil, ywang@yucca.nrl.navy.mil

ABSTRACT

We apply a tracking technique, previously developed to study motions in the outer corona by Sheeley, Walters, Wang, and Howard, to 195 Å filtergrams obtained with the *Transition Region and Coronal Explorer* (*TRACE*) satellite and obtain height-time maps of the motions in the hot (10–20 MK) plasma clouds above postflare loop systems. These maps indicate the following two main characteristics. (1) Within the plasma cloud, the motions are downward at speeds of approximately 4 km s^{-1}. The cloud itself grows with time, its upper layers being replenished by the arrival and deceleration of fast inflows and its lower layers disappearing when they cool to form the tops of new postflare loops. (2) Early in these events, the inward motions are turbulent, showing a variety of dark elongated features resembling ''tadpoles'' and some bright features. Later, the inflows are visible as dark collapsing loops, changing from initially cusp-shaped features to rounder loops as they move inward. Their speeds initially lie in the range 100–600 km s^{-1} but decrease to 4 km s^{-1} in about 3 minutes, corresponding to an average deceleration ∼1500 m s^{-2}. Combining these observations with similar observations obtained at reconnection sites in the outer corona by the Large Angle Spectrometric Coronagraph (LASCO), we conclude that postflare loops are the end result of the formation, filling, deceleration, and cooling of magnetic loops produced by the reconnection of field lines blown open in the flare. The formation of collapsing loops occurs in the dark tadpoles; the filling of these initially dark loops occurs via chromospheric evaporation, which also contributes to the deceleration of the loops; and the radiative cooling ultimately resolves the loops into sharply defined structures.

Subject headings: interplanetary medium — Sun: activity — Sun: corona — Sun: magnetic fields

1. INTRODUCTION

Large solar flares begin when magnetic field lines are blown open to form transient coronal holes (Rust 1983; Sterling & Hudson 1997). These empty regions fill in during the declining phase of the flares as sequences of progressively larger postflare loops become visible in low-temperature chromospheric and coronal emission lines (Bruzek 1964; Sheeley et al. 1975; Svestka 1976, pp. 42–48; Harvey et al. 1986). According to current ideas, the newly opened magnetic field lines reconnect to form loops that are subsequently filled by chromospheric evaporation from their footpoints (Carmichael 1964; Sturrock 1966; Neupert 1968; Hudson 1973; Kopp & Pneuman 1976; Antiochos & Sturrock 1978). These loops radiatively cool and eventually become visible in low-temperature emission lines (Forbes & Acton 1996; Warren et al. 1999). Because radiative cooling is especially effective at the lower temperatures, individual loops are seen for only a few minutes, and the postflare loop system is the rising locus of the newly filled loops that are currently visible at the temperature of observation. Even at chromospheric temperatures, the newly formed loops fade quickly as material drains down the legs in the form of ''coronal rain'' (Tandberg-Hanssen 1977).

This paper presents a new analysis of *Transition Region and Coronal Explorer* (*TRACE*) observations above postflare loop systems and of Large Angle Spectrometric Coronagraph (LASCO) observations at warped sector boundaries in the outer corona. Taken separately, each set of observations provides convincing evidence that the observed inflows indicate magnetic field line reconnection. Taken together, the observations allow us to construct a detailed and consistent picture of the closing-down of flux at current sheets.

In § 2.1 we present height-time maps that show the motions in the plasma clouds above postflare loops. As we shall see,

these maps indicate that all of the physical elements above the postflare loop system, including elongated dark ''tadpoles,'' dark loops, and the bright elements of the cloud itself, move downward while the boundary of the cloud expands upward in a wavelike manner. In § 2.2 we use LASCO observations to clarify the nature of the dark tadpoles and to deduce their relationship to the collapsing loops and cusps. Finally, in § 3 we summarize our observational findings and provide a physical interpretation for them.

2. OBSERVATIONS

2.1. *TRACE Observations*

In the first three panels of Figure 1, the *TRACE* images of the west limb event on 2002 April 21 illustrate the basic components of a postflare loop system. The postflare loops themselves are visible in the lower left corner of each image as bright strands of 1.6 MK emission from a blend of Fe xii lines in the bandpass of the 195 Å filter. Above these loops, a hot plasma cloud is visible in 10–20 MK emission from the Fe xxiv 192 Å line that also lies within the passband of the filter. Some dark, finger-like features are visible probing into the plasma cloud from above. Such dark ''tadpoles'' have been reported previously for this flare (Gallagher et al. 2002; Innes et al. 2003a, 2003b; Sheeley & Wang 2002; Seaton et al. 2003) and for the 2002 July 23 east-limb flare (Asai et al. 2004), as well as for several flares observed with the Soft X-ray Telescope (SXT) on the *Yohkoh* satellite (McKenzie & Hudson 1999; McKenzie 2000) and the Soft X-ray Imager (SXI) on the National Oceanic and Atmospheric Administration (NOAA) *GOES-12* satellite (Hill 2004). Consequently, such inflows are now thought to be essential components of the decay phase of large solar flares.

The fourth panel is a difference image, obtained by subtracting the image shown in the third panel from one taken a
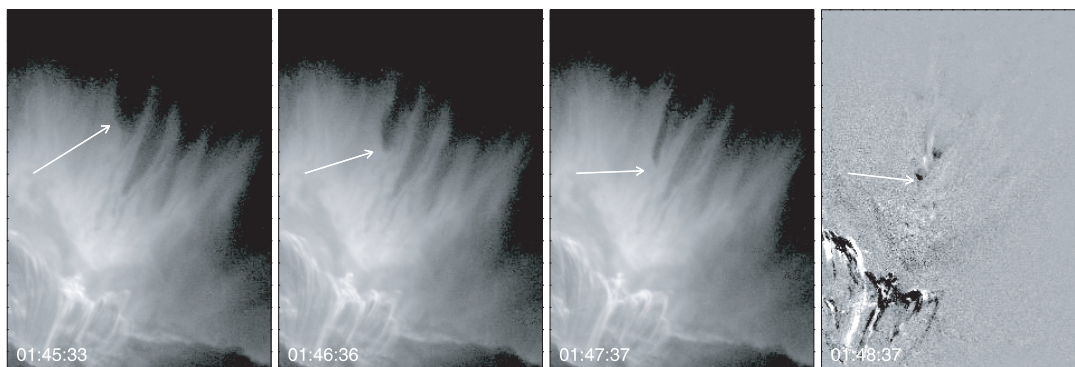
Fig. 1.—*TRACE* 195 Å filtergrams of the 2002 April 21 west-limb flare showing Fe xii postflare loops (*lower left*) and the Fe xxiv plasma cloud (*center*) penetrated by dark tadpole-like inflows (*upper right*). The fourth panel is a difference image showing the change between the images at 0147 and 0148 UT. These images have been rotated so that the solar limb is approximately horizontal. The arrow refers to a "tadpole" whose height-time track is indicated in Fig. 2. The vertical dimension of each panel is approximately 117 Mm.

minute later. Such difference images indicate changes without the distracting effects of the more slowly evolving background and provide a sensitive way of revealing motions of faint coronal features. Here the inflow marked by the arrow is being overtaken by another inflow coming in from above. In this paper we shall use sequences of such running difference images to study the motions above postflare loops.

The top panel of Figure 2 shows the motions that occurred along the path of the inflow indicated in Figure 1 during 0103–0223 UT, and the bottom panel shows motions along a nearby path without such "tadpoles" during this time. These maps were made from consecutive "running difference" images (like that in the fourth panel of Fig. 1) by adapting the technique that Walters

developed to study motions in the outer corona (Sheeley et al. 1999). Narrow strips along the path of interest were selected and placed in chronological order to obtain a rectangular display of the difference signal as a function of time (horizontal axis) and distance along the path (vertical axis).

The top panel of Figure 2 shows tracks of the rapidly decelerating inflows, the gradually settling plasma cloud, and the gradually rising postflare loops. At the greatest height, the tracks of a "tadpole" (*arrow*) slope steeply downward at first and then fall quickly in line with several other much less inclined tracks. The speed began at 250 km s^{-1} but decelerated to 5 km s^{-1} after 3.2 minutes, corresponding to an average deceleration of 1300 m s^{-2}. These values are typical of the *TRACE* inflows that
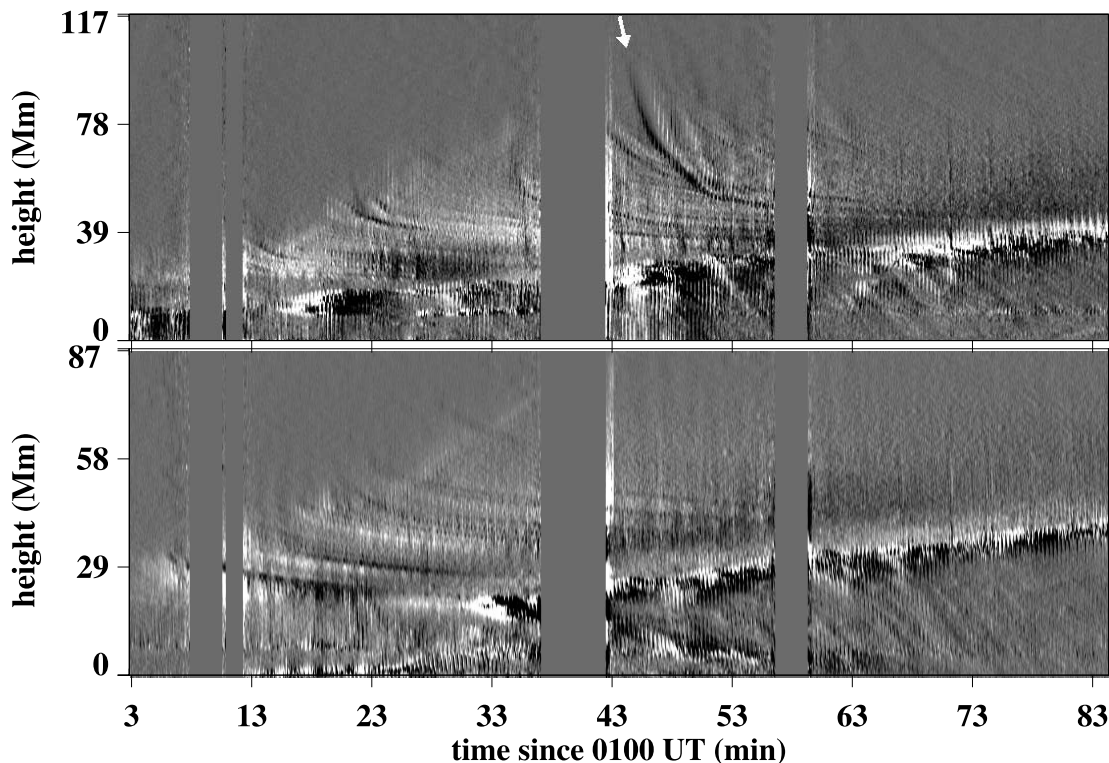
April 21, 2002

Fig. 2.—Height-time maps for two paths through the plasma cloud in Fig. 1. The top panel was obtained for the path of the "tadpole" (arrow in Fig. 1) and shows steep tracks rapidly decelerating to form new layers of the slowly descending cloud. The bottom panel shows a neighboring region without "tadpoles" and emphasizes the relation between the descending tracks of the plasma cloud and the rising ramp of postflare loops.
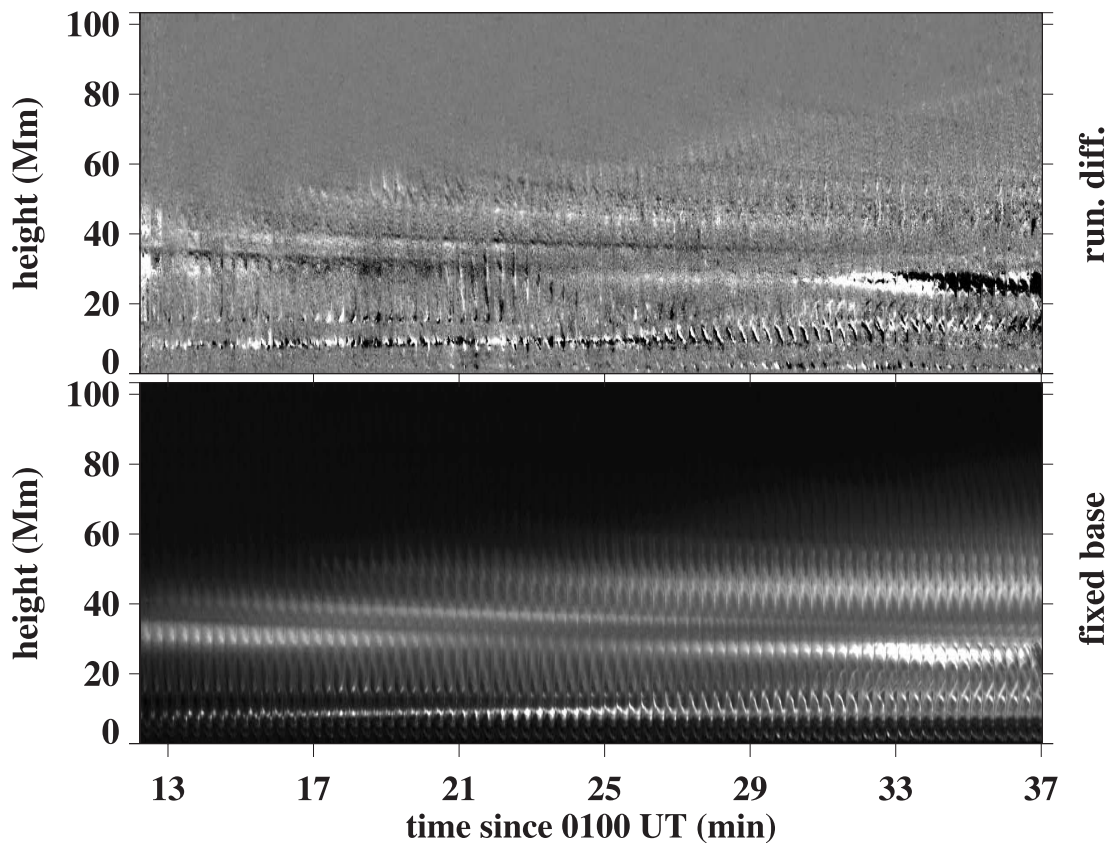
April 21, 2002 (w = 25)

Fig. 3.—Enlargement of a section of the bottom panel of Fig. 2 showing the height-time tracks in running difference images (*top panel*) and in difference images expressed relative to a fixed image at the start of the panel (*bottom panel*). The fixed-base map shows that the postflare loops at 0133 UT can be tracked back into the plasma cloud. In this figure and later ones, "w" refers to the width of the slit (in pixels) used to make the height-time map.

we have measured for the flares on 2002 April 21 and July 23 and 2003 November 4.

At intermediate heights, the less inclined tracks form a layered region slanting downward very slightly at 4–5 km s^{-1}. This region corresponds to the hot plasma cloud in Figure 1. The individual layers fade briefly before arriving at the rising locus of the postflare loop system. We suppose that this momentary decrease of visibility indicates that the plasma is passing through the $\sim$4 MK temperature region where it is too cool to produce Fe XXIV emission but too hot to produce Fe XII emission. Its faint signal may correspond to emission in the relatively weaker Ca XVII 193 Å line. Eventually, the downward slanting layers terminate at the ($\sim$7 km s^{-1}) rising locus of the postflare loop system.

The bottom panel of Figure 2 provides another view of this layered region with new tracks coming in from progressively greater heights. Here the rising postflare loop system begins with the arrival of the oldest track of the plasma cloud. In the lower right, one can barely see fainter and steeper tracks of falling material beneath the postflare loop system. Their speeds of $\sim$60 km s^{-1} are consistent with the reported speeds of "coronal rain," which falls down the legs of postflare loops at 50–100 km s^{-1} (Tandberg-Hanssen 1977) and is quite different from the $\sim$4 km s^{-1} inward motion of the plasma cloud.

Figure 3 provides even more direct evidence that the postflare loops form from the cooling elements of the plasma cloud. The top panel is an enlargement of the bottom panel of Figure 2 during 0113–0137 UT and shows several downward tracks as

they approach the postflare loop system. The bottom panel is made from difference images expressed relative to a fixed-base frame at the start of the panel and shows the elements of the cloud essentially as they appear against the sky. Here we can see that the bright region of newly formed postflare loops at 0133–0137 UT maps backward in time through a short gap at 0121–0125 UT to a bright streak at 0113–0121 UT. Evidently, as the temperature cooled, the unresolved Fe XXIV loops faded, producing the gap (where they are weakly visible in Ca XVII emission at 4 MK), and then brightened again when they reached the Fe XII temperature near 1.6 MK. In this map, a similar track is visible in the next (higher) layer of the cloud. Such detailed correspondences leave no doubt that the postflare loops form from the inbound elements of the cloud.

Not all of the fast inflows are shaped like tadpoles. The running difference images in Figure 4 show several loop-shaped features moving inward toward a postflare loop system at the west limb on 2003 November 4. These loops have a leading-black/trailing-white signature, which means that, like the "tadpoles," they would appear as dark features surrounded by a brighter coronal background when observed in unsubtracted images. The loop marked by the arrow has the height-time track shown in the top panel of Figure 5. It evolves from a tall pointed structure to a short rounder one as if the tension in the loop were decreasing with time. Its leading-black/trailing-white signature is clearly visible. A quadratic fit to this height-time track gives an initial speed of 125 km s^{-1} and a deceleration of 690 m s^{-2}, corresponding to a decay time of 3.0 minutes.

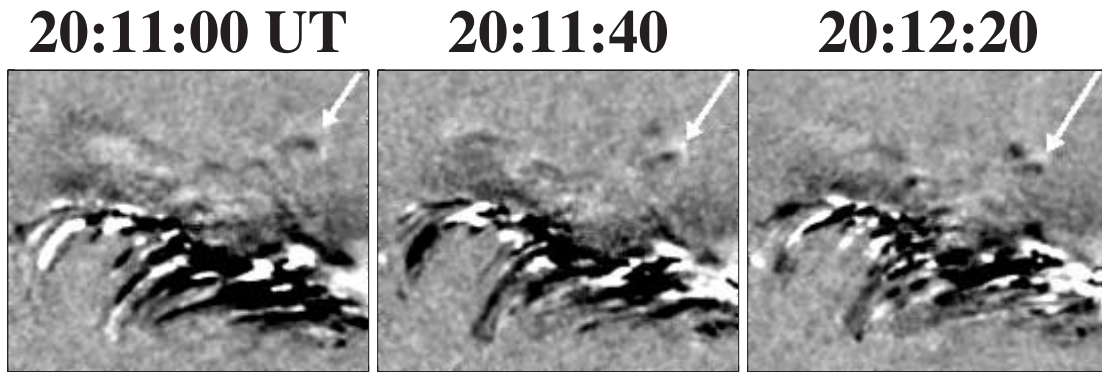## 20:11:00 UT   20:11:40   20:12:20

FIG. 4.—A sequence of *TRACE* running difference images on 2003 November 4 showing several collapsing loops above a postflare loop system at the west limb. The arrow indicates a collapsing loop whose height-time track is indicated in the top panel of Fig. 5. The vertical dimension of each panel is approximately 54 Mm. To capture the faint background features, we combined the relatively underexposed frames in a 20 s interval around each time of interest before subtracting to form the running difference images.

The lower panel of Figure 5 shows an even more striking example of the change from a pointed loop to a rounder one, again with the leading-black/trailing-white signature of a dark loop seen against a brighter background. A quadratic fit to this profile gives a starting speed of 255 km s^{-1} and a deceleration of 1150 m s^{-2}, corresponding to a decay time of 3.7 minutes.

These properties of the collapsing loops are consistent with what one might expect from the reconnection of open magnetic field lines high above the flare site. Their initial speeds are large (100–600 km s^{-1} based on all of our measurements), their initial shapes are cusplike, and they are darker than their surroundings. This suggests that the reconnection occurs where the density is too low to keep the oppositely directed field lines apart and that the dark loops are newly reconnected flux tubes that have not yet filled with plasma.

Why do the inflows appear as tadpoles on 2002 April 21 but as dark collapsing loops on 2003 November 4? A possible clue is provided by Figure 6, which shows observations during the 2002 July 23 east-limb flare. Early in the event (*top panel*), the height-time map shows several tracks moving inward through a brightening background, similar to the brightening plasma cloud on April 21 (cf. Fig. 2). The tracks are complicated. Most of them are composed of dark, tadpole-shaped features and some are bright, but none of them has the signature of a collapsing loop. However, the background stops brightening toward the end of the panel, and 15 minutes later the bottom panel shows the first of several collapsing loops. This loop is similar to those observed on 2003 November 4 (cf. Fig. 5); it has the running difference signature of a dark loop against a bright background, and its speed decreases from 190 to 60 km s^{-1} in 3 minutes, corresponding to an average deceleration of 700 m s^{-2}. Because a bright but unchanging background intensity ought to reveal dark tadpoles as well as dark collapsing loops, we doubt that the distinction is a visibility
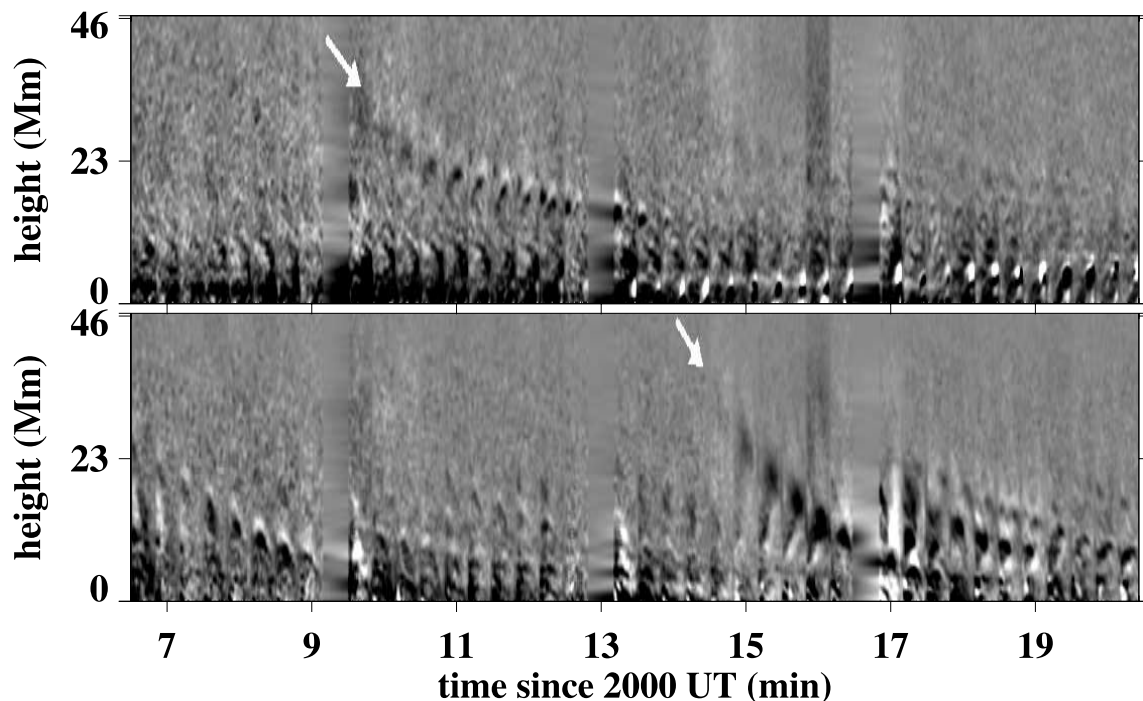
November 4, 2003   (w = 25)

FIG. 5.—Height-time maps for two paths through the region above the 2003 November 4 postflare loop system. The arrows indicate tracks of collapsing loops that become less stretched out as they decelerate.

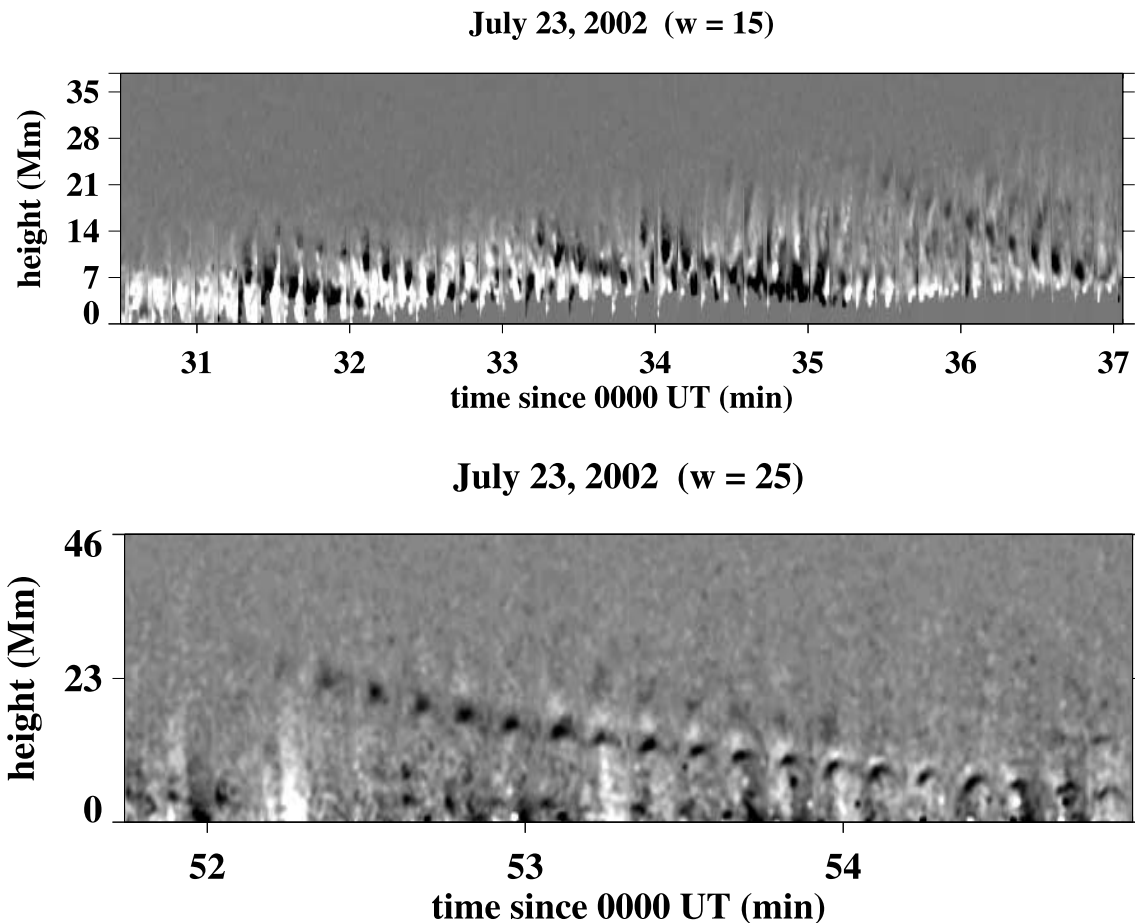## July 23, 2002 (w = 15)

July 23, 2002 (w = 25)

FIG. 6.—Height-time maps of *TRACE* running difference images comparing inflows at two times during the 2002 July 23 east-limb flare. In the earlier map (*top panel*), a variety of dark tadpole-like features penetrate a brightening plasma cloud above the (occulted) postflare loops. In the later map (*bottom panel*), a single collapsing loop shows the leading-black/trailing-white difference signature of a loop that is darker than its surroundings when seen against the sky.

effect related to the brightening background. Instead, we suppose that the distinction is related to the nature of the reconnection during the early and late stages of the flare event.

Our confidence in this conclusion is bolstered by the LASCO observations, which show thousands of inflow events with a variety of tadpoles and collapsing loops. Next, we examine some of these LASCO observations.

2.2. *LASCO Observations*

The upper two panels of Figure 7 show tadpoles observed with the LASCO coronagraph on 2001 July 24 about 24 hr after a major coronal mass ejection (CME) occurred at this limb position. The first height-time map was made from difference images expressed relative to the same fixed-base image near the start of the sequence and shows the inflows approximately as they appear against the sky. These LASCO inflows appear as dark tadpoles pushing their way into the rising material $2-4\,R_{\odot}$ from the Sun at speeds on the order of 75–100 km s^{-1}. This is characteristic of the LASCO tadpoles; they are enhanced by the bright material they encounter, either by moving into denser regions or by being deflected from their predominantly radial paths in collisions with stationary features or outward ejections. (For further examples, see Wang et al. 1999; Sheeley et al. 2001; Sheeley & Wang 2001.) The second height-time map was made from running difference images and shows three downward tracks similar to those seen in the top panel of Figure 6.

In the lower panel, the LASCO height-time map shows a collapsing loop at the east limb on 2002 December 6–7. It was

one of about 70 inflows that were observed as a warp in the streamer belt rotated past the limb. A quadratic fit to this track gives an initial speed of 90 km s^{-1} and a deceleration of 2.6 m s^{-2}, corresponding to a decay time of 9.7 hr. These values are representative of many LASCO inflows, whose maximum speeds lie in the range 60–100 km s^{-1} and whose decelerations take several hours.

Although some LASCO observations show either tadpoles or loops, many other observations show both features as separate stages of the same event (Sheeley & Wang 2002). Figure 8 describes one of these prototype inflows during the west-limb passage of a sector boundary on 2000 October 23. The height-time map in the top panel was made from running difference images and shows an initial acceleration followed by a deceleration. Fitting this track with a cubic polynomial, we obtained a maximum speed of 60 km s^{-1} and endpoint accelerations of ± 4.8 m s^{-2}. (A quadratic fit gives a starting speed of 70 km s^{-1} and a constant deceleration of 1.9 m s^{-2}, corresponding to a decay time of 10.2 hr.)

Near 1000 UT, when the speed obtained its maximum value, the running difference signature changed from black to leading-black/trailing-white. This means that the inflow began as a density discontinuity with the less-dense region (a depletion tail) trailing behind the more-dense region. Such depletion tails are relatively difficult to see against the dark sky far from the Sun. Consequently, the discontinuity appears as the top of a sinking column of bright emission. However, as the discontinuity moves inward, the dark tail becomes more visible and the sinking
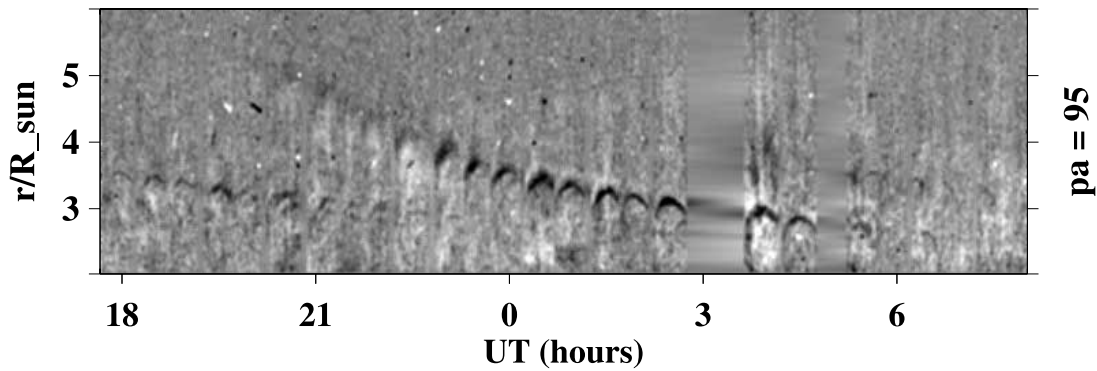
JULY 24, 2001
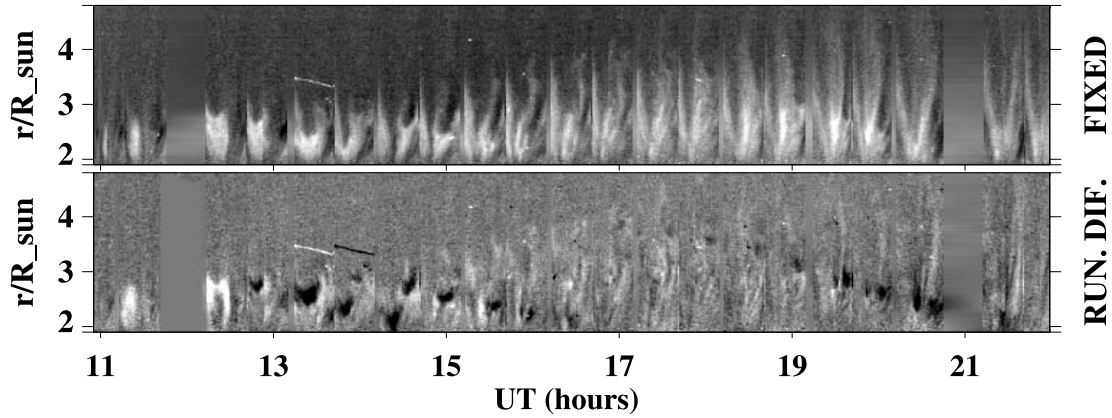
December 6 - 7, 2002

FIG. 7.—LASCO height-time maps showing "tadpoles" (*top panels*) and loops (*bottom panel*) moving inward through the corona. In the top panels, the map made from running difference images shows three dark tracks moving downward through a faintly brightening background; the companion map was made from difference images relative to a fixed-base frame at the start of the map and shows the dark tadpoles plunging into the rising bright background intensity, as they would appear against the sky. In this figure and in Fig. 8, "pa" refers to the orientation (position angle in degrees counterclockwise from solar north) of the slit used to make the height-time map.
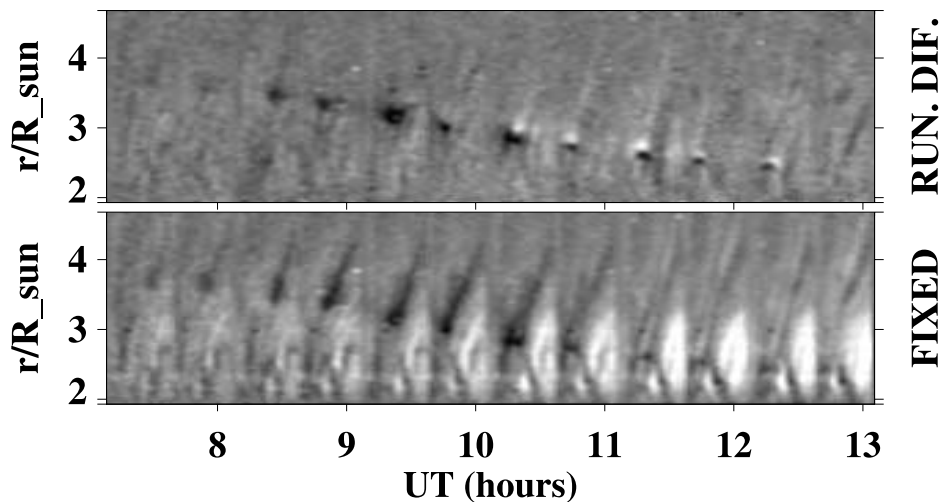
October 23, 2000   (pa = 258, w = 25)

FIG. 8.—Height-time maps of a typical LASCO inflow during the west-limb passage of a warped sector boundary. *Top panel*: Running difference images showing the transition from a pure black signal to a leading-black/trailing-white signal; *bottom panel*: fixed-base images showing the growth of a dark depletion tail whose sudden disappearance corresponds to the transition in the top panel. We think that the loss of the depletion tail and the formation of the collapsing loop are indications that the reconnection is over.

column becomes lost in the brighter background material closer to the Sun.

In running difference images, the transition from a black signature to a leading-black/trailing-white signature can only happen if the inflow sheds its elongated depletion tail and becomes an isolated dark feature (which, in the upper panel of Figure 8, seems to be a small loop). In the lower panel of Figure 8, the height-time map is made from fixed-base difference images and shows the depletion tail and dark loop directly as they appear against the sky (but with much greater visibility than is possible with unsubtracted images). As expected, the dark tail disappeared around 1000 UT when the height-time track in the upper panel changed its character, and a small isolated dark feature (evidently an unresolved loop) survived to extend the track past 1200 UT.

Many such LASCO observations led us to conclude that the field-line reconnection occurs in the dark tail where the density is too low to keep the oppositely directed field lines apart (Sheeley & Wang 2002). In this case, the loss of the tail and the surviving dark cusp-shaped loop might indicate that all of the field lines in the tail have been pinched off and that the reconnection is finished.

If this scenario applies to the *TRACE* observations, then the tadpoles must be depletion tails where field lines are still reconnecting. By comparison, the collapsing dark loops without tails would be signs that the reconnection is finished. This hypothesis is consistent with *TRACE* observations of the 2002 July 23 east-limb flare, in which the dark tadpoles occurred early in the event and collapsing dark loops occurred later when we might expect the reconnection to be coming to an end.

3. DISCUSSION

3.1. *Summary of Observations*

The *TRACE* observations show that on 2002 April 21, the postflare loop system was covered by a rising cloud of falling elements. The upper layers were replenished as high-speed inflows moved into the cloud and decelerated, and the lower layers disappeared at the location of newly forming postflare loops. The inflows had initial speeds in the range 100–600 km s^{-1} and decelerated in about 3 minutes, corresponding to an average value of about 1500 m s^{-2}. They were darker than their surroundings and were shaped like tadpoles swimming toward the Sun. Observations late in the 2003 November 4 west-limb flare revealed collapsing dark loops with pointed tops that became rounder with time. Observations on 2002 July 23 showed tadpoles early in the event when the background intensity was increasing and collapsing dark loops later. As the falling elements of the plasma cloud cooled, their intensity changed from bright (Fe XXIV emission at 10–20 MK) to relatively faint (weaker Ca XVII emission at 4 MK) and then again to bright (Fe XII emission at 1.6 MK), when they were briefly visible as well-defined postflare loops.

LASCO observations at warped sector boundaries showed similar dark tadpoles and collapsing loops, often as separate phases of the same inflow event. The tadpoles were enhanced during encounters with dense material, either ejected from the Sun or simply blocking their inward motion. The depletion tails eventually disappeared and were replaced by dark cusps that changed to rounded loops as they moved inward. The maximum speeds were in the range 50–100 km s^{-1}, and the decelerations took $\sim$8 hr, corresponding to values $\sim$2 m s^{-2}.

3.2. *Interpretation*

Based on the *TRACE* observations, we suppose that the hot plasma cloud consists of unresolved loops, which cool as they move downward and eventually become recognized as postflare loops when they reach the 1.6 MK temperature of the Fe XII lines used for observation. We have known for some time that hot loops are fuzzier than cold ones (Tousey et al. 1973), and it is plausible that a collection of loops would be unrecognizably blurred together at the 10–20 MK temperature of Fe XXIV emission. Conversely, we might expect a collection of cooling loops to become resolved at lower temperatures where the much greater radiative cooling rate would allow fewer loops to be seen at any given time (Warren et al. 1999; Patsourakos et al. 2004a, 2004b, in preparation). Based on the lengths of gently sloping tracks in Figure 2, we estimate a cooling time of about 30–40 minutes for the newly filled loops to reach the 1.6 MK temperature of Fe XII emission.

It is significant that all of the internal elements of the cloud move downward while the outer boundary of the cloud expands upward away from the Sun. This means that the upward motion must be a wave, like the rising locus of postflare loops, and not a true motion of the unresolved loops within the cloud. We would expect such a wavelike motion from a rising reconnection point, similar to that of Kopp & Pneuman (1976), which continually releases new loops into the collapsing pile.

It is also significant that the high-speed inflows that enter the cloud are dark. As discussed previously for the LASCO data (Sheeley & Wang 2002), this suggests that the reconnection occurs where the density is too low to keep the oppositely directed field lines apart. The reconnection sites are elongated depletion tails (the "tadpoles"), with empty loops moving forward and eventually becoming visible as dark cusp-shaped features when the tail is pinched off. If such empty loops are to become filled, the material must come from their ends back at the Sun, presumably via chromospheric evaporation (Tandberg-Hanssen & Emslie 1988, p. 212, and references therein). In this scenario, the outward components would remain dark and unobserved because their ends are detached from the Sun.

Numerical simulations (Nagai & Emslie 1984; Mariska et al. 1989) indicate that such loops should become filled in an evaporation time τ_e given by

$$\tau_e \sim L/v_s, \qquad (1)$$

where L is the loop length (roughly twice its height) and v_s is the sound speed of the plasma in the loop. Adopting $L = 120$ Mm from Figure 2 and estimating $v_s = 500$ km s^{-1} for a 15 MK plasma, we obtain a value of $\tau_e \sim 240$ s = 4 minutes. This value is comparable to the $\sim$4 minute formation time of each new layer of the plasma cloud, estimated from the bottom panel of Figure 3. It is also comparable to the 3 minute deceleration time required to bring the high-speed tadpoles and collapsing loops to rest in the sinking cloud. These estimates raise the question of whether the evaporation itself may be responsible for the deceleration by providing an upward force analogous to that obtained by inflating a balloon.

We can test this idea by making similar estimates for the LASCO inflows. Using a loop length $L \sim 4\ R_\odot$ and a sound speed $v_s \sim 120$ km s^{-1} for a 1 MK plasma, we obtain an "evaporation" time $\tau_e \sim 6.5$ hr. This value lies well within the range of times that the LASCO inflows take to decelerate and disappear into the background corona. The agreement is particularly encouraging when one realizes that these deceleration times are 2 orders of magnitude larger than those obtained for the *TRACE* inflows.

There are two additional reasons for supposing that the filling of the loops would have an appreciable effect on their

deceleration. First, the plasma pressures appear sufficient to balance the magnetic energy density in the fields. For the *TRACE* observations (Warren et al. 1999), a density $n \gtrsim 5 \times 10^{10}$ cm^{-3} and a temperature $T \sim 15 \times 10^6$ K in the hot plasma clouds give a pressure $n\kappa T \sim 10^{-3}$ ergs cm^{-3}, roughly equivalent to that of a 50 G field and larger than the 15–30 G fields that one expects 60 Mm above a large $\sim 10^{22}$ Mx active region. Similarly, for the LASCO observations an electron density $n_e \sim 10^6$ cm^{-3} and temperature $T \sim 1 \times 10^6$ K at 2.5 $R_\odot$ correspond to a plasma pressure $2n_e\kappa T \sim 3 \times 10^{-4}$ ergs cm^{-3}, equivalent to that of a 0.1 G field. This field strength is approximately the value one obtains from the outward extrapolation of a 2 G photospheric field or the inward extrapolation of a 5×10^{-5} G interplanetary field at Earth. Thus, the estimated plasma and magnetic pressures are comparable in the region 2–2.5 $R_\odot$ from Sun center where the transition between open and closed coronal structures is observed.

Second, numerous LASCO height-time maps like that in Figure 8 show that the deceleration begins at the transition point where the inflow loses its depletion tail and the collapsing loop is formed (see also Sheeley & Wang 2002). Thus, the formation of the loop seems to be a signal for the deceleration to begin. We have previously noted that the smooth, oscillation-free deceleration requires more than a balance between the downward magnetic tension and upward magnetic compression in the newly reconnected loop (Sheeley & Wang 2002), and it now seems possible that the inflation of the loop may provide the required upward force.

We summarize our interpretation as follows. The reconnection begins after the field lines are opened and the outflow of plasma stops. Then the oppositely directed field lines in this low-density region start to pinch off and release newly reconnected loops that are not visible against the dark sky. The outward components escape unseen, but the inward components become filled with hot (10–20 MK) material that is evaporated from the chromosphere in $\sim$4 minutes. This bright cloud of unresolved loops provides a background for observing subsequent depletion tails and dark collapsing loops. As the reconnection point moves outward, the cloud expands, but its individual (largely unresolved) loops all move downward at $\sim$4 km s^{-1} as they cool. After 30–40 minutes, individual loops

reach temperatures of 1.6 MK and become visible in Fe XII emission as familiar postflare loops. But they are quickly lost again as the plasma continues to cool and as material drains down their legs in the form of "coronal rain." The next generation of loops forms at a slightly greater height, causing the Fe XII locus to rise at about 7 km s^{-1}.

In retrospect, we can identify several observational milestones that led to this interpretation. The first milestone was the recognition that the LASCO and *TRACE* inflows are similar. This led to the idea that we were seeing a universal signature of coronal field-line reconnection, which could be used to interpret *TRACE* observations from LASCO data and vice versa. It also made us realize that the inflows and the hot plasma cloud are not separate components of the flare but that the cloud is produced by the same kinds of dark inflows that it eventually made visible. The second milestone was the construction of the *TRACE* height-time maps. The rising cloud of falling elements meant that the upward motion was a wave, consistent with a rising point of reconnection. And the downward tracks, terminating at the locus of the rising postflare loops, meant that these loops originated in the cloud. The third milestone was the discovery of a transition time when the LASCO inflows lost their depletion tails and turned into cusp-shaped collapsing dark loops. This suggested that the reconnection occurred in the depletion tail and was therefore over when the tail was pinched off. The fourth milestone was the measurement of the *TRACE* decelerations. This allowed a quantitative comparison of the loop filling times and led to the idea that the inflation of the loops may contribute to the deceleration of both the *TRACE* and LASCO inflows.

REFERENCES

Antiochos, S. K., & Sturrock, P. A. 1978, ApJ, 220, 1137
Asai, A., Yokoyama, T., Shimojo, M., & Shibata, K. 2004, ApJ, 605, L77
Bruzek, A. 1964, ApJ, 140, 746
Carmichael, H. 1964, in The Physics of Solar Flares, ed. W. N. Hess (NASA SP-50; Washington: NASA), 451
Forbes, T. G., & Acton, L. W. 1996, ApJ, 459, 330
Gallagher, P. T., Dennis, B. R., Krucker, S., Schwartz, R. A., & Tolbert, K. 2002, Sol. Phys., 210, 341
Harvey, K. L., Sheeley, N. R., Jr., & Harvey, J. W. 1986, in Solar-Terrestrial Predictions, ed. P. A. Simon, G. Heckman, & M. A. Shea (Boulder: NOAA), 198
Hill, S. M. H. 2004, BAAS, 204, 02.09
Hudson, H. S. 1973, in High Energy Phenomena on the Sun, ed. R. Ramaty & R. G. Stone, (NASA SP-342; Washington, DC: NASA), 207
Innes, D. E., McKenzie, D. E., & Wang, T. 2003a, Sol. Phys., 217, 247
———. 2003b, Sol. Phys., 217, 267
Kopp, R. A., & Pneuman, G. W. 1976, Sol. Phys., 50, 85
Mariska, J. T., Emslie, A. G., & Li, P. 1989, ApJ, 341, 1067
McKenzie, D. E. 2000, Sol. Phys., 195, 381
McKenzie, D. E., & Hudson, H. S. 1999, ApJ, 519, L93
Nagai, F., & Emslie, A. G. 1984, ApJ, 279, 896
Neupert, W. M. 1968, ApJ, 153, L59

Patsourakos, S., Antiochos, S. K., & Klimchuk, J. A. 2004a, ApJ, 614, 1022
Rust, D. 1983, Space Sci. Rev., 34, 21
Seaton, D. B., DeLuca, E. E., Cooper, F. C., & Nakariakov, V. M. 2003, BAAS, SPD 34, 16.18
Sheeley, N. R., Jr., Knudson, T. N., & Wang, Y.-M. 2001, ApJ, 546, L131
Sheeley, N. R., Jr., Walters, J. H., Wang, Y.-M., & Howard, R. A. 1999, J. Geophys. Res., 104, 24739
Sheeley, N. R., Jr., & Wang, Y.-M. 2001, ApJ, 562, L107
———. 2002, ApJ, 579, 874
Sheeley, N. R., Jr., et al. 1975, Sol. Phys., 45, 377
Sterling, A. C., & Hudson, H. S. 1997, ApJ, 491, L55
Sturrock, P. 1966, Nature, 211, 695
Svestka, Z. 1976, Solar Flares (Dordrecht: Reidel)
Tandberg-Hanssen, E. 1977, in Illustrated Glossary for Solar and Solar-Terrestrial Physics, ed. A. Bruzek & C. J. Durrant (Dordrecht: Reidel), 97
Tandberg-Hanssen, E., & Emslie, A. G. 1988, The Physics of Solar Flares (Cambridge Univ. Press: New York)
Tousey, R., et al. 1973, Sol. Phys., 33, 265
Wang, Y.-M., Sheeley, N. R., Jr., Howard, R. A., St. Cyr, O. C., & Simnett, G. M. 1999, Geophys. Res. Lett., 26, 1203
Warren, H. P., Bookbinder, J. A., Forbes, T. G., Golub, L., Hudson, H. S., Reeves, K., & Warshall, A. 1999, ApJ, 527, L121